Electronic Supplementary Information

Highly efficient silica coated perovskite nanocrystals with the assistance of ionic liquid for warm white LEDs

Yanqiao Xu,*‡[a,b] Xiaobo Hu,‡[c] Huidong Tang,[b] Qing Hu,[b] Sanhai Wang,[b] Ting Chen,[a] Xiaojun Zhang,[a,b] Weihui Jiang,[a,b] Lianjun Wang,*[c] and Wan Jiang[c]

[a]National Engineering Research Center for Domestic & Building Ceramics, Jingdezhen Ceramic Institute, Jingdezhen 333000, China

[b]School of Material Science and Engineering, Jingdezhen Ceramic Institute, Jingdezhen 333000, China

[c]State Key Laboratory for Modification of Chemical Fibers and Polymer Materials College of Materials Science and Engineering, Donghua University, Shanghai 201620, China

*Corresponding Authors. Emails: xuyanqiao@jcu.edu.cn (Y. X.); wanglj@dhu.edu.cn (L. W.)

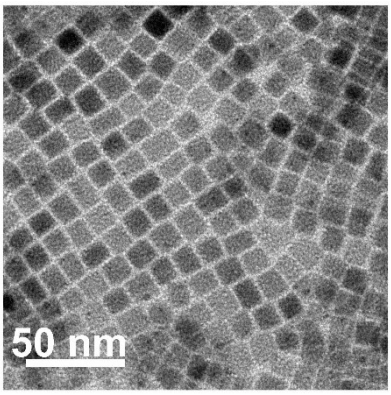

Fig. S1 TEM image of $CsPbBr_3$ NCs.

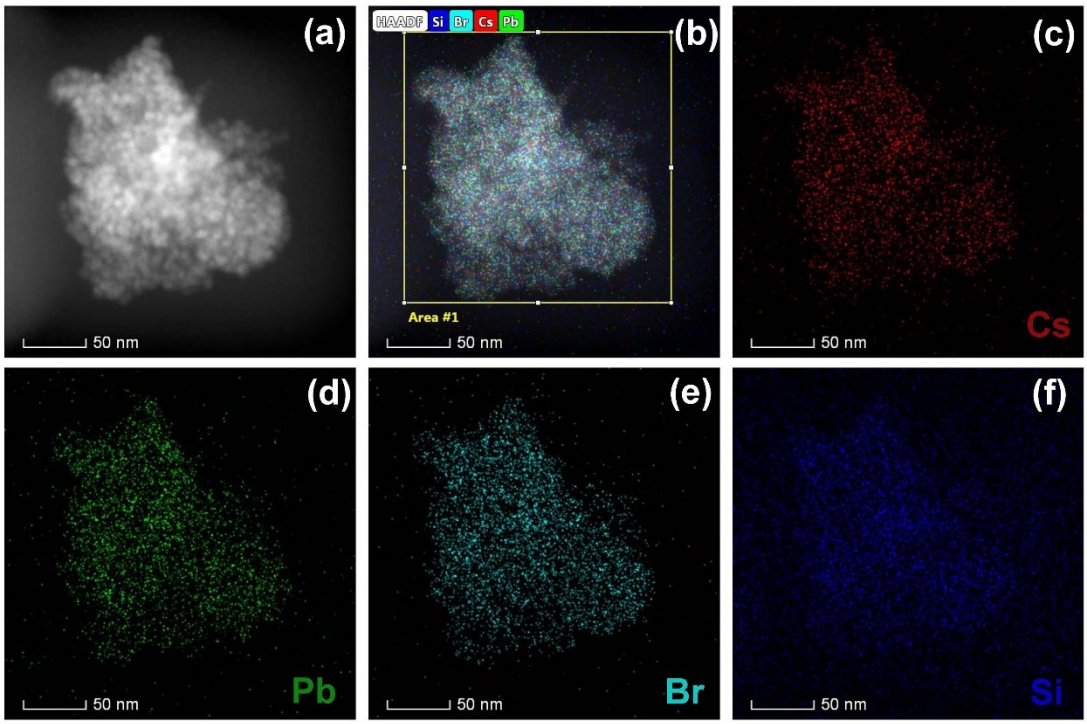

Fig. S2 (a) HAADF-STEM image and (b-f) elemental maps of $CsPbBr_3$@SiO_2 NCs.

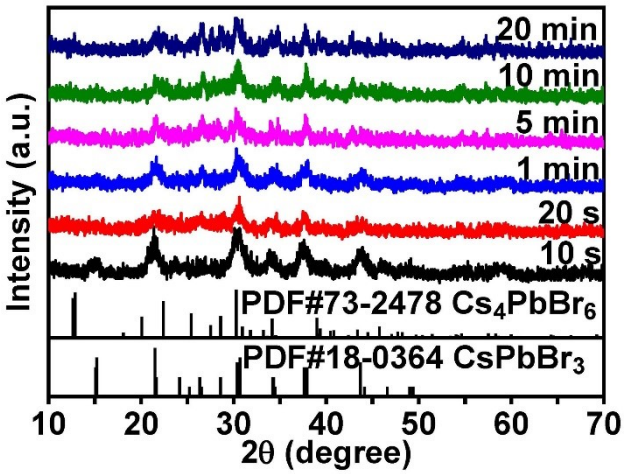

Fig. S3 XRD patterns of $CsPbBr_3$@SiO_2 NCs prepared with different hydrolysis time of APTES.

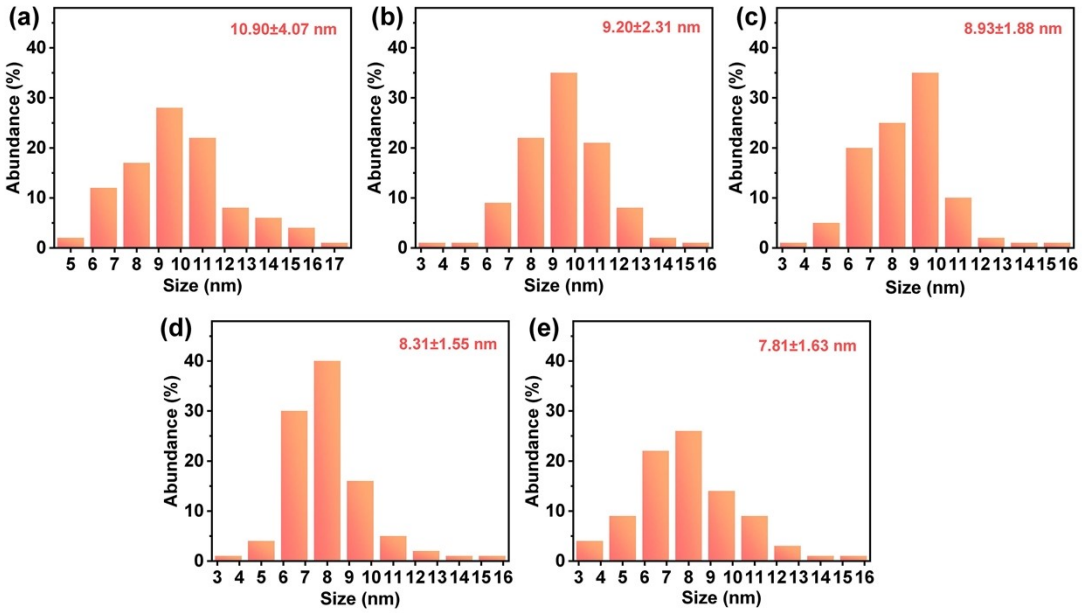

Fig. S4 Size distribution histograms of $CsPbBr_3$ cores prepared with hydrolysis time of (a) 10 s, (b) 20 s, (c) 1 min, (d) 5 min, and (e) 10 min.

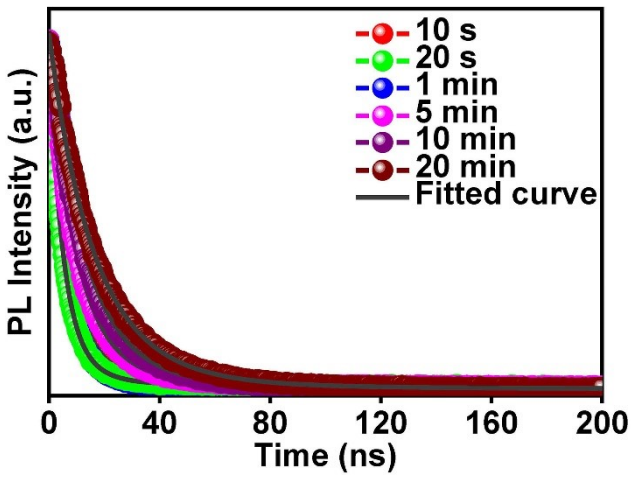

Fig. S5 Decay curves of $CsPbBr_3$@SiO_2 NCs prepared with different hydrolysis time of APTES.

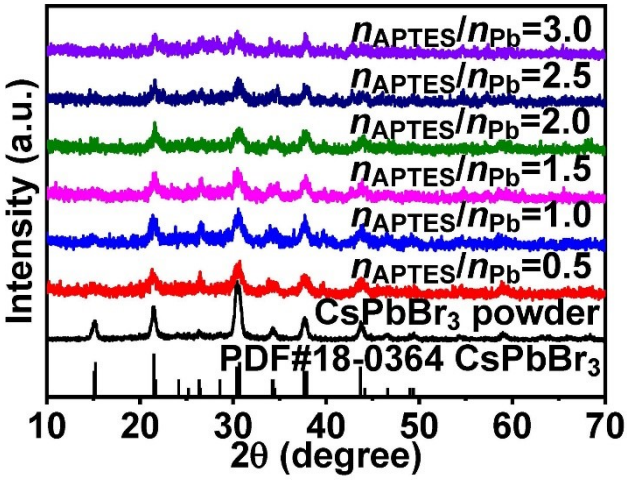

Fig. S6 XRD patterns of $CsPbBr_3$@SiO_2 NCs prepared by one-step method with different n_{APTES}/n_{Pb} ratios (Adding APTES into anti-solvent).

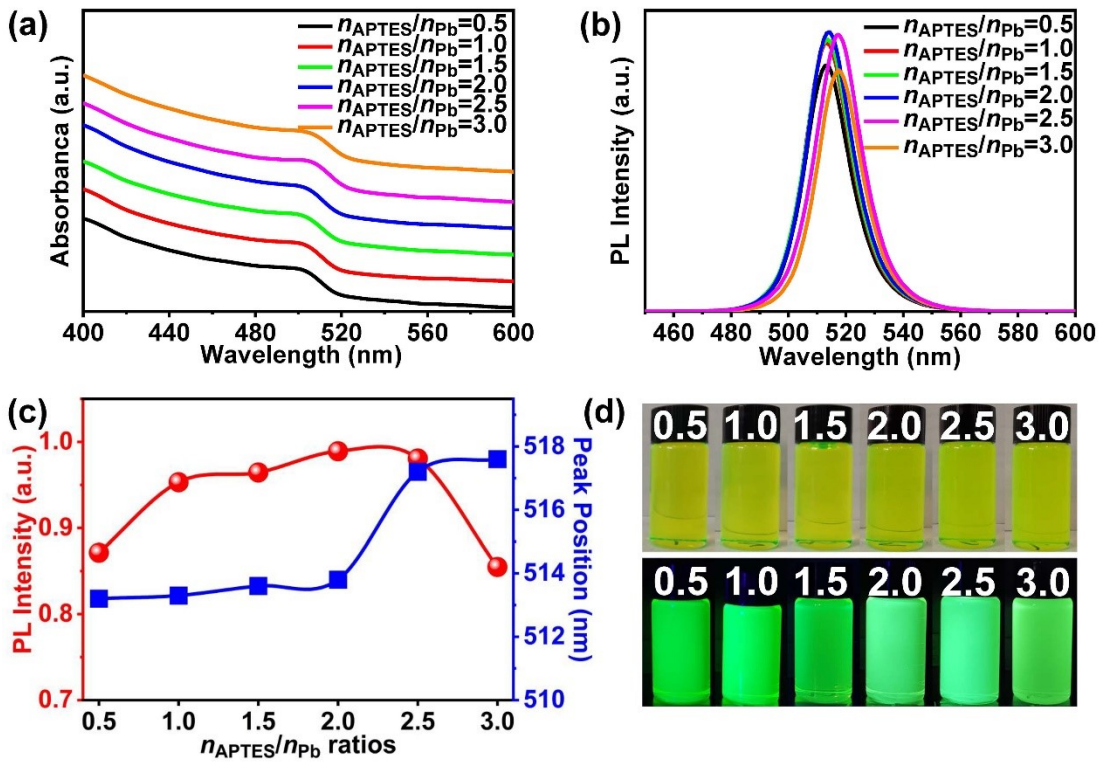

Fig. S7 (a) Absorption, (b) emission spectra, (c) evolution of emission intensity and peak position of $CsPbBr_3$@SiO_2 NCs prepared by one-step method with different n_{APTES}/n_{Pb} ratios, and (d) photos of samples under sunlight and UV light (Adding APTES into anti-solvent).

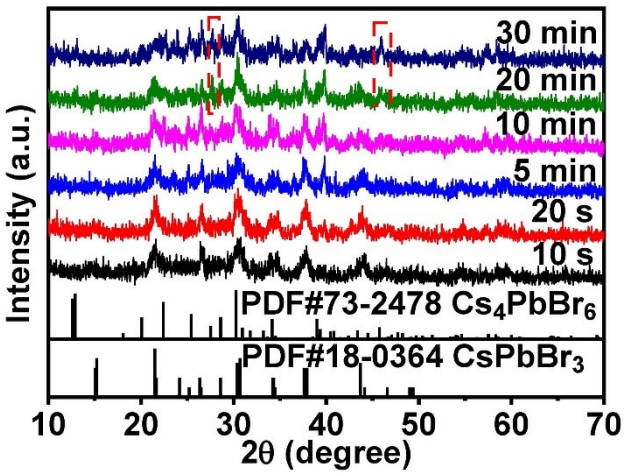

Fig. S8 XRD patterns of $CsPbBr_3$@SiO_2 NCs prepared by one-step method with different reaction time (Adding APTES into anti-solvent).

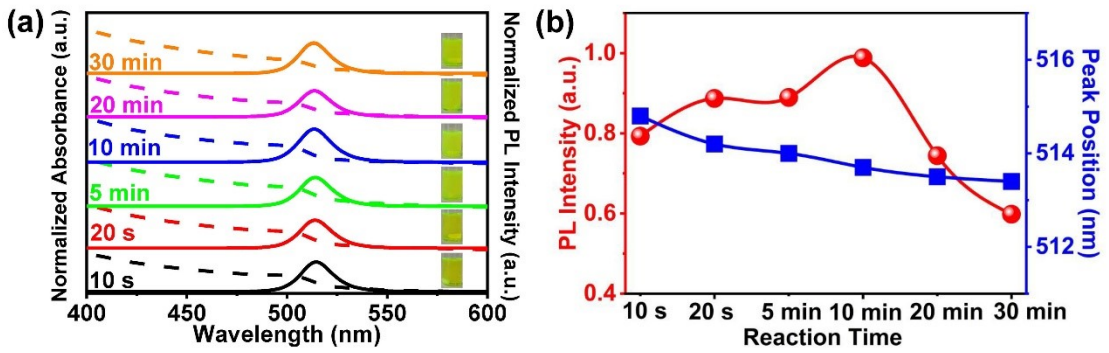

Fig. S9 (a) Absorption and emission spectra, and (b) evolution of emission intensity and peak position of $CsPbBr_3$@SiO_2 NCs prepared by one-step method with different reaction time (Adding APTES into anti-solvent).

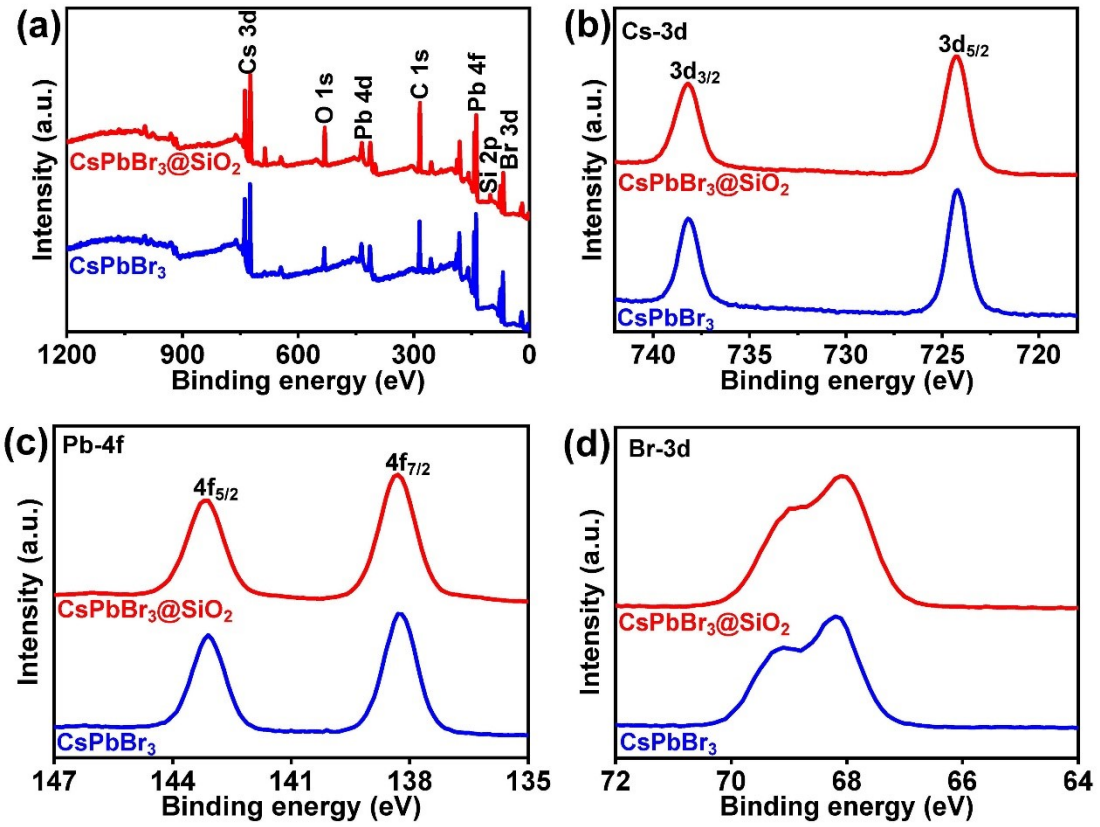

Fig. S10 (a) XPS survey spectra, and XPS element analysis of (b) Cs-3d, (c) Pb-4f, (d) Br-3d, (e) N-1s, and (f) Si-2p of $CsPbBr_3$ NCs and $CsPbBr_3$@SiO_2 NCs.

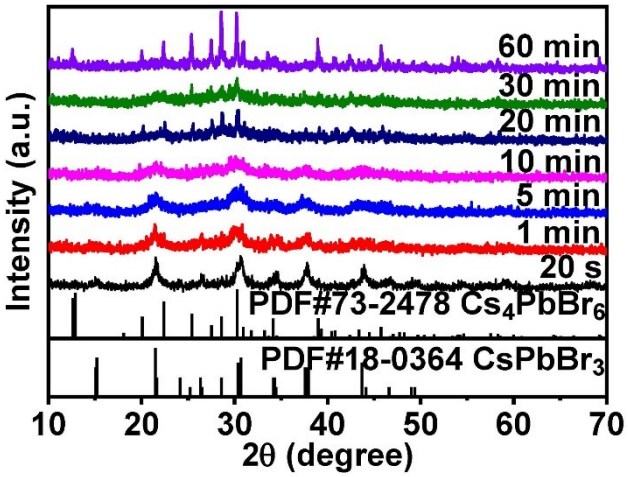

Fig. S11 XRD patterns of $CsPbBr_3@SiO_2$ NCs prepared with different reaction time (Without adding IL).

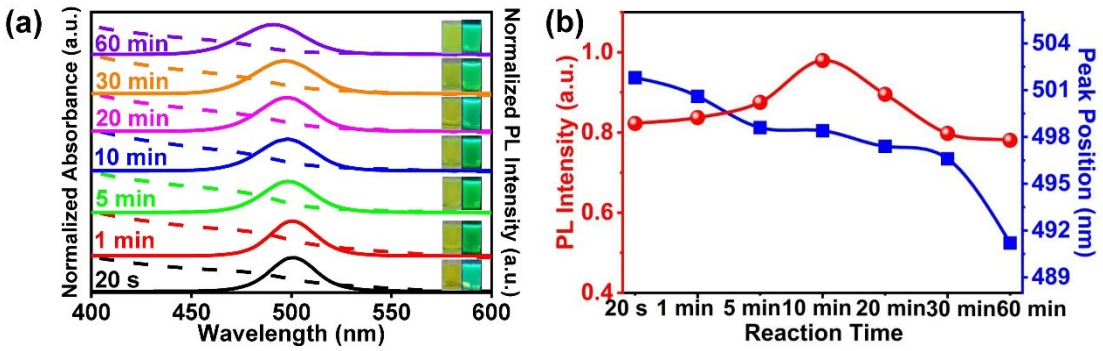

Fig. S12 (a) Absorption and emission spectra, and (b) evolution of emission intensity and peak position of $CsPbBr_3@SiO_2$ NCs prepared with different reaction time (Without adding IL).

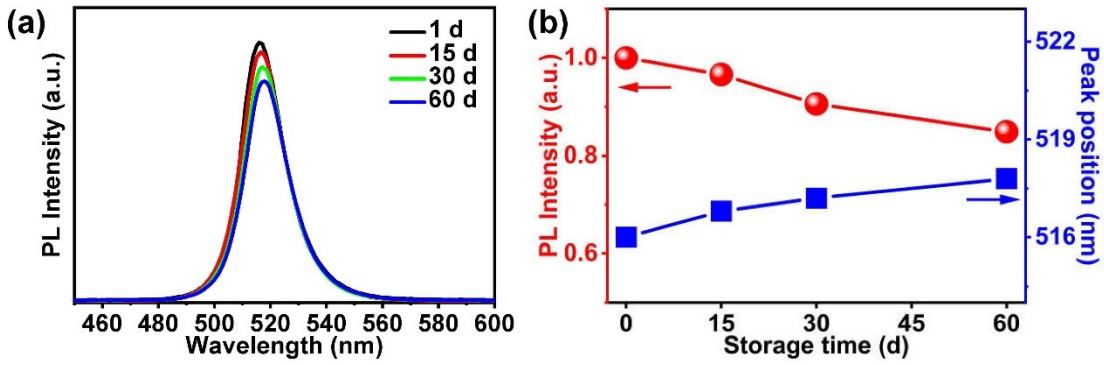

Fig. S13 Storage stability test results of $CsPbBr_3$ NCs.

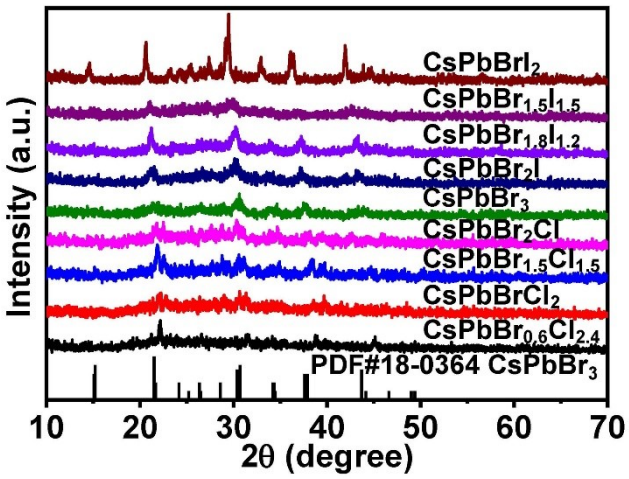

Fig. S14 XRD patterns of $CsPbX_3$@SiO_2 NCs.

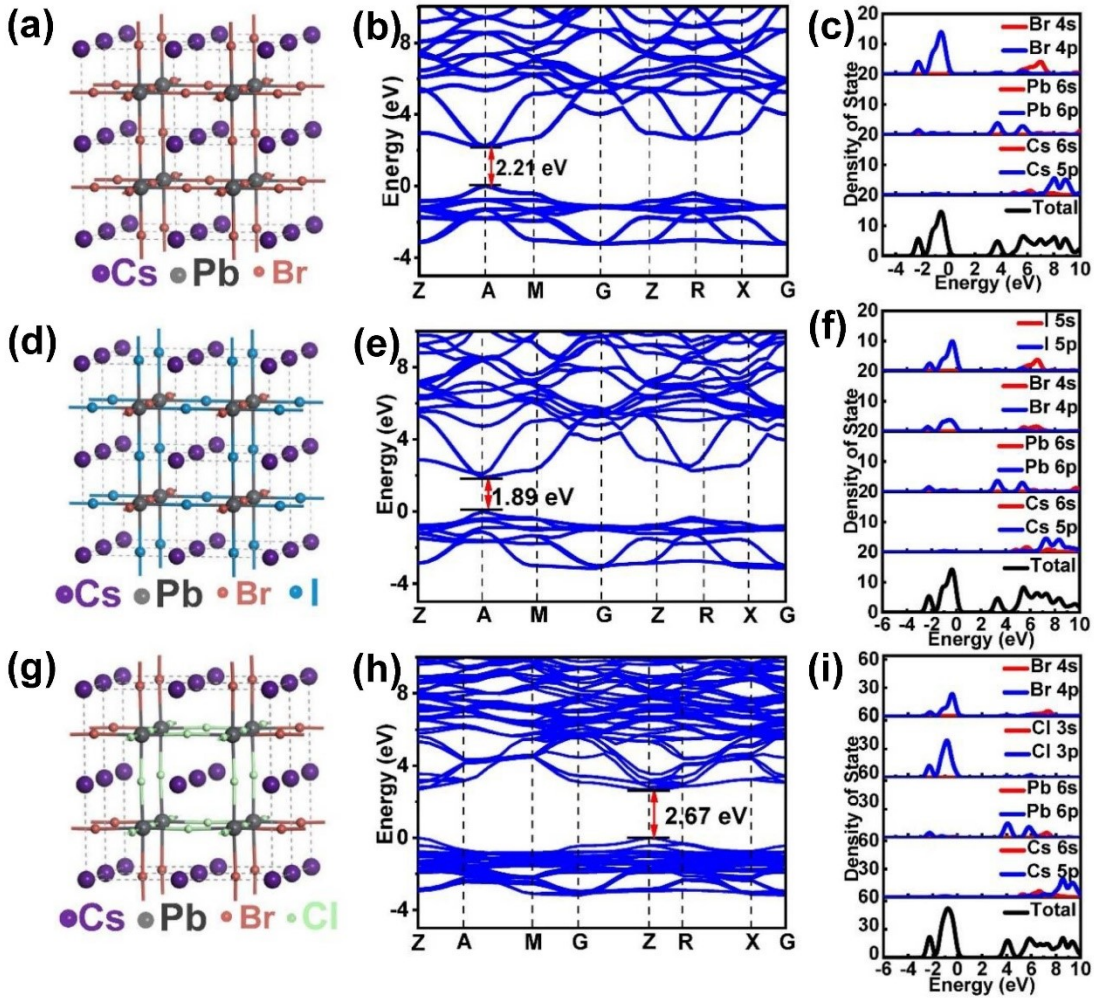

Fig. S15 Optimized structures, calculated electronic band structures and density of state of (a-c) $CsPbBr_3$, (d-f) $CsPbBrI_2$, and (g-i) $CsPbBrCl_2$.

The theoretical calculations were carried out using Cambridge Serial Total Energy Package (CASTEP) based on plane-wave pseudo-potential.[1] Generalized gradient approximation of Perdew-Burke-Ernzerhof (PBE) was adopted for the exchange-correlation functional.[2] The Monkhorst 2×2×2 grim was used for $CsPbX_3$ and the E_{cut} was set as 300 eV. Structure relaxation was stopped until the force of each atom was less than 0.01 eV/Å. The optimized structures, calculated electronic band structures, and density of state of $CsPbBr_3$, $CsPbBrI_2$, and $CsPbBrCl_2$ were shown in Fig. S15. It was found that the conduction band of $CsPbBr_3$ was composed

of 6p orbital of Pb atoms, while the valance band was formed by the antibonding interaction between Br 4p and Pb 6s states due to the strong hybridization (Fig. S15c). Moreover, the 3p orbital of Cl atoms or 5p orbital of I atoms involved in the formation of valance band when partial Br was replaced with Cl or I (Fig. S15(f) and (i)). The calculated bandgap of $CsPbBr_3$, $CsPbBrI_2$, and $CsPbBrCl_2$ was 2.21 eV, 1.89 eV, and 2.67 eV, respectively.

Table S1 The performances of silica coated perovskite NCs

Samples	Silicon source	Reaction time	PLQY	Ref
$CH_3NH_3PbBr_3@SiO_2$	TMOS[a]	36 h	87%	Huang et al [3]
$CsPbBr_3@SiO_2$	TMOS	12 h	65%	Li et al. [4]
$CsPbBr_3@SiO_2$	APTES[b]	3 h	78%	Sun et al. [5]
$CsPbBr_3@SiO_2$	TMOS	24 h	73.4%	Zhang et al. [6]
$CsPbBr_3@SiO_x$	TEOS	10 h	–	Park et al. [7]
$CsPbBr_3@SiO_2$	TMOS	12 h	80%	Hu et al. [8]
$CsPbBr_3@SiO_2$	APTES[c]	20 s	85.7%	This work

[a] tetramethyl orthosilicate; [b] (3-aminopropyl)triethoxysilane; [c] tetraethyl orthosilicate.

Table S2 Fitting results of PL decay curves of $CsPbBr_3@SiO_2$ NCs prepared with different n_{APTES}/n_{Pb} ratios

n_{APTES}/n_{Pb}	τ_1/ns	B_1/%	τ_2/ns	B_2/%	χ^2	τ_{av}/ns
0	10.13	91.28	60.20	8.72	0.9955	28.26
1.0	5.28	93.77	50.72	6.23	0.9990	22.98
1.5	6.14	96.91	26.04	3.09	0.9995	8.51
2.0	6.14	98.51	34.77	1.49	0.9996	8.40
2.5	16.88	95.01	62.31	4.99	0.9994	24.26
3.0	14.02	93.33	47.84	6.67	0.9994	20.65

Table S3 Fitting parameters of PL decay curves of $CsPbBr_3@SiO_2$ NCs prepared with different hydrolysis time of APTES

Time	τ_1/ns	B_1/%	τ_2/ns	B_2/%	χ^2	τ_{av}/ns
10 s	6.53	97.95	24.40	2.05	0.9996	7.83
20 s	5.95	99.05	34.21	0.95	0.9995	7.43
1 min	6.14	98.51	34.77	1.49	0.9996	8.40
5 min	10.19	97.11	74.75	2.89	0.9994	21.76
10 min	13.13	96.61	65.37	3.39	0.9993	20.90
20 min	17.91	94.64	64.12	5.36	0.9995	25.70

Table S4 Calculation results of VBM and CBM values of $CsPbX_3$ NCs and SiO_2

Samples	VBM/eV	Optical bandgap/eV	CBM/eV
$CsPbBr_{0.6}Cl_{2.4}$	-6.322	3.046	-3.276
$CsPbBrCl_2$	-6.284	2.894	-3.390
$CsPbBr_2Cl$	-6.170	2.696	-3.474
$CsPbBr_3$	-5.916	2.360	-3.556
$CsPbBr_2I$	-5.881	2.258	-3.623
$CsPbBrI_2$	-5.558	1.912	-3.646
SiO_2	-8.435	8.600	0.165

References

1 M. D. Segall, P. J. D. Lindan, M. J. Probert, C. J. Pickard, P. J. Hasnip, S. J. Clark and M. C. Payne, First-principles simulation: ideas, illustrations and the CASTEP code, *J. Phys.: Condens. Matter*, 2002, **14**, 2717–2744.

2 J. P. Perdew, K. Burke and M. Ernzerhof, Generalized gradient approximation made simple, *Phys. Rev. Lett.*, 1996, **77**, 3865–3868.

3 S. Huang, Z. Li, L. Kong, N. Zhu, A. Shan and L. Li, Enhancing the stability of $CH_3NH_3PbBr_3$ quantum dots by embedding in silica spheres derived from tetramethyl orthosilicate in “waterless” toluene, *J. Am. Chem. Soc.*, 2016, **138**, 5749–5752.

4 M. Li, X. Zhang and P. Yang, Controlling the growth of a SiO_2 coating on hydrophobic $CsPbBr_3$ nanocrystals towards aqueous transfer and high luminescence, *Nanoscale*, 2021, **13**, 3860–3867.

5 C. Sun, Y. Zhang, C. Ruan, C. Yin, X. Wang, Y. Wang and W. W. Yu, Efficient and stable white LEDs with silica-coated inorganic perovskite quantum dots, *Adv.*

Mater., 2016, **28**, 10088–10094.

6 L. Zhang, Y. Xie, Z. Tian, Y. Liu, C. Geng and S. Xu, Thermal conductive encapsulation enables stable high-power perovskite-converted light-emitting diodes, *ACS Appl. Mater. Interfaces*, 2021, **13**, 30076–30085.

7 S. Park, M. N. An, G. Almeida, F. Palazon, D. Spirito, R. Krahne, Z. Dang, L. D. Trizio and L. Manna, $CsPbX_3/SiO_x$ (X= Cl, Br, I) monoliths prepared via a novel sol-gel route starting from Cs_4PbX_6 nanocrystals, *Nanoscale*, 2019, **11**, 18739–18745.

8 H. Hu, L. Wu, Y. Tan, Q. Zhong, M. Chen, Y. Qiu, D. Yang, B. Sun, Q. Zhang and Y. Yin, Interfacial synthesis of highly stable $CsPbX_3$/oxide Janus nanoparticles, *J. Am. Chem. Soc.*, 2018, **140**, 406–412.